Tephra transformations: variable preservation of tephra layers from two well-studied eruptions

Bulletin of Volcanology

Tephra transformations: variable preservation of tephra layers from two well-studied eruptions
--Manuscript Draft--

Manuscript Number:	BUVO-D-18-00053R3
Full Title:	Tephra transformations: variable preservation of tephra layers from two well-studied eruptions
Article Type:	Research Article
Corresponding Author:	Nick A Cutler, Ph.D Newcastle University Newcastle upon Tyne, Tyne and Wear UNITED KINGDOM
Corresponding Author Secondary Information:	
Order of Authors:	Nick A Cutler, Ph.D
	Richard T Streeter
	Joseph Marple
	Lauren R Shotter
	Jean S Yeoh
	Andrew J Dugmore
Funding Information:	National Science Foundation (1202692) — Prof Andrew J Dugmore National Science Foundation (1249313) — Prof Andrew J Dugmore

Abstract:	Volcanologists often use terrestrial tephra layers to reconstruct volcanic eruptions. However, the conversion of fresh tephra deposits into tephra layers is poorly understood. To address this knowledge gap, we surveyed tephra layers emplaced by the 1980 eruption of Mount St Helens, USA (MSH1980) and the 1947 eruption of Hekla, Iceland (H1947). We compared our measurements with observations made shortly after the 1947 and 1980 eruptions, to calibrate the subsequent transformation of the tephra deposit. We expected the tephra layers to retain the broad characteristics of the original deposits, but hypothesized a) changes in thickness and mass loading due to re-working, and b) positive correlations between thickness and vegetation density. We observed some systematic changes in tephra layer properties with distance from the vent and the main plume axis. However, the preservation of the layers varied both between and within our survey locations. Closed coniferous forest appeared to provide good conditions for the preservation of the MSH1980 tephra, as expected; preservation of the H1947 deposit in sparsely vegetated parts of Iceland was much more variable. However, preservation of the MSH1980 deposit in sparsely vegetated areas of eastern Washington State was also excellent, possibly due to biocrust formation. We concluded that the preservation of tephra layers is sensitive to surface conditions at the time of the eruption. These findings have implications for the reconstruction of past eruptions where eruption plumes span regions of variable surface cover.

Response to Reviewers:	Minor editorial changes completed
Author Comments:	Minor editorial changes completed

1   **Tephra transformations: variable preservation of tephra layers from**

2   **two well-studied eruptions**

3

4   Cutler, N.A.[1]; Streeter, R.T.[2], Marple, J.[2], Shotter, L.R.[3], Yeoh, J.S.[3], Dugmore, A.J. [3, 4, 5]

5

6   [1] School of Geography, Politics & Sociology, Newcastle University, UK

7   [2] School of Geography & Sustainable Development, University of St Andrews, UK

8   [3] School of Geosciences, University of Edinburgh, UK

9   [4] Department of Anthropology, Washington State University, USA

10   [5] Graduate Center, City University of New York, USA

11

12   Corresponding author:

13   Nick A Cutler, School of Geography, Politics & Sociology, 5th Floor Claremont Tower,

14   Newcastle University, Newcastle upon Tyne, NE1 7RU, UK

15   Email: nick.cutler@ncl.ac.uk

16

17   **Abstract**

18   Volcanologists often use terrestrial tephra layers to reconstruct volcanic eruptions.

19   However, the conversion of fresh tephra deposits into tephra layers is poorly

20   understood. To address this knowledge gap, we surveyed tephra layers emplaced by

21   the 1980 eruption of Mount St Helens, USA (MSH1980) and the 1947 eruption of Hekla,

22   Iceland (H1947). We compared our measurements with observations made shortly after

23   the 1947 and 1980 eruptions, to calibrate the subsequent transformation of the tephra

24   deposit. We expected the tephra layers to retain the broad characteristics of the original

25   deposits, but hypothesized a) changes in thickness and mass loading due to re-working,

26   and b) positive correlations between thickness and vegetation density. We observed

27   some systematic changes in tephra layer properties with distance from the vent and the

28   main plume axis. However, the preservation of the layers varied both between and

29   within our survey locations. Closed coniferous forest appeared to provide good

30   conditions for the preservation of the MSH1980 tephra, as expected; preservation of the

31   H1947 deposit in sparsely vegetated parts of Iceland was much more variable.

32   However, preservation of the MSH1980 deposit in sparsely vegetated areas of eastern

33   Washington State was also excellent, possibly due to biocrust formation. We concluded

34   that the preservation of tephra layers is sensitive to surface conditions at the time of the

35   eruption. These findings have implications for the reconstruction of past eruptions where

36   eruption plumes span regions of variable surface cover.

37

38   Key words: Hekla; Mount St Helens; mass loading; biocrusts; kriging; volcanological

39   reconstruction; biophysical feedbacks

Introduction

Layers of tephra preserved in soils are frequently used in the reconstruction of past volcanic eruptions and the evaluation of volcanic hazards (Houghton and Carey 2015). For example, tephra layers may be used to estimate the total volume of pyroclastic material erupted, eruption intensity, column height and the spatial distribution of pyroclastic deposits (Bonadonna and Houghton 2005; Pyle 1989). Inferences based on terrestrial tephra layers have greatly extended the short and rather patchy record of volcanic eruptions based on historical accounts, and made a major contribution to our understanding of volcanism (Lowe 2011). However, they rely on the assumption that the preserved tephra layer is representative of the initial deposit. A great deal can happen to tephra after deposition and the ways in which tephra layers are preserved (or not) are poorly understood (Fig. 1). The formation of tephra layers is difficult to observe directly, as it can be lengthy (unfolding over years to decades) and spatially variable. Furthermore, tephra deposited on land is vulnerable to post-depositional re-working by wind, water and slope processes: in the worst-case scenario, all of the deposited tephra can be lost to erosion (Blong et al. 2017; Pyle 2016). Surface characteristics, notably vegetation cover, can also influence preservation (Cutler et al. 2016a; Cutler et al. 2016b; Dugmore et al. 2018). These factors impose a limit on the information that a tephra layer can provide. Clearly, a deposit that has been extensively re-worked is an unreliable indicator of eruption parameters, but it is often unclear how representative ancient, apparently unmodified, tephra layers are.

[Fig. 1: tephra preservation]

63

64   One way to address the knowledge gap surrounding tephra layer preservation is to

65   record the physical characteristics (typically layer thickness, mass per unit area (mass

66   loading), and internal stratigraphy) of a tephra layer and to compare this record with

67   similar measurements made shortly after an eruption. In this way, it should be possible

68   to calibrate the degree of physical transformation that a tephra deposit undergoes

69   during preservation, i.e., the process by which it is incorporated into the sedimentary

70   record over a timescale of decades or longer (it is possible that buried layers may still

71   undergo modification). If the tephra deposit crosses ectones (the transitional regions

72   between distinctive vegetation types, e.g., the boundary between forest and savanna), it

73   should also be possible to investigate the influence of vegetation cover on tephra

74   preservation. To do this, we compared relatively thin (<10 cm) preserved tephra layers

75   from two twentieth century volcanic events – the eruptions of Hekla in 1947 (H1947)

76   and Mount St Helens in 1980 (MSH1980) - with measurements of the tephra deposits

77   taken shortly after the eruptions (i.e., prior to incorporation into the stratigraphic record).

78   Relatively thin tephra layers may be lost in some depositional environments (e.g., due to

79   chemical weathering), but persist in many settings to form an important record of past

80   eruptions.

81

82   We expected the tephra layers to capture the overall features of the original deposit. For

83   example, we anticipated that layer thickness and mass loading would, on the whole,

84   decrease with a) distance from the vent and b) distance from the main axis of the

85   eruption plume (Houghton and Carey 2015). With MSH1980 we expected to find an

86   area of distal secondary thickening described in contemporary reports (Sarna-Wojcicki

87   et al. 1981). However, we also expected transformation of the deposit to varying

88   degrees. We used our results to test two hypotheses:

89

90   H1: The preserved tephra layer would be thinner than the initial deposit due to

91   compaction and/or the loss of material due to reworking by wind, water and slope

92   processes; mass/unit area would only be lower due to losses.

93   H2: Tephra layer thickness would vary according to vegetation cover, with the highest

94   levels of tephra retention (relative to the original deposit) in the areas of densest

95   vegetation (e.g., closed forest) and the lowest in areas of sparse vegetation cover.

96

97

98   **Methods**

99

100   The study areas

101   We chose the MSH1980 and H1947 tephra layers because the eruptions that produced

102   them were the subject of detailed, contemporaneous studies (refer to Online Resource

103   1 for details of the historical datasets we used in this study). Both were plinian eruptions

104   that distributed tephra over 1000s of km^2 (Table 1, Figs 2, 3). Crucially, records of initial

105   tephra depth and mass loading, each based on dozens of measurements taken shortly

106   after the eruptions, have been published (Thorarinsson 1954; Waitt and Dzurisin 1981).

107   In the case of MSH1980, some of the researchers who monitored the eruption were still

108   active when we were carrying out the study, and we were able to conduct fieldwork in

109   collaboration with one of them (Dr Richard Waitt of the USGS). The eruptions are

110   sufficiently recent that vegetation cover in the fallout zones has not changed

111   dramatically (based on photographic evidence). Conversely, the time that has elapsed

112   between the original surveys and our measurements (H1947: 70 years, MSH1980: 35

113   years) is sufficient to ensure the burial of the layers.

114

115   [Table 1: characteristics of the MSH1980 and H1947 eruptions]

116

117   We focused our study on areas > 15 km from the vent that received relatively thin initial

118   deposits (~10 cm or less). These areas were spatially extensive and we reasoned that

119   records of the fallout would be numerous and comparatively reliable (as the accurate

120   recording of very thin (sub-mm) and very thick (multiple metre) deposits in the field is

121   challenging: Yang and Bursik 2016). We collected data on tephra thickness and mass

122   loading, two variables used in reconstructions of volcanic eruptions. In the case of the

123   MSH1980 layer, we also recorded the internal stratigraphy in locations within 50 km of

124   the vent. Grain size distribution is another important characteristic of tephra layers.

125   However, a sparsity of tabulated data and major differences between the methodologies

126   and statistics reported in the literature meant it was not possible to make meaningful

127   comparisons between original and recent grain size distributions.

128

129   [Fig. 2: Fallout map: MSH1980]

130   [Fig. 3: Fallout map: H1947]

131   [Fig. 4: Illustrative photos of the three different environments]

132

133 We screened the original datasets and removed the following data points:

134 • All zero values, because our study focused on $\log_{10}$ thickness and we were not

135 concerned with establishing the edge of the fallout zone;

136 • Values from locations close to the vent (within a few km), as these are often highly

137 variable, due to partial column collapse and uneven topography (Yang and Bursik

138 2016);

139 • Values we judged to be unreliable due to uncertain provenance (H1947 dataset

140 only: refer to Online Resource 1).

141 This left samples sizes of n = 163 for MSH1980 and n= 62 for H1947.

142

143 Clearly, there is likely to be a small degree of uncertainty in the measurements

144 themselves: Engwell et al. (2013) estimated observational error in the measurement of

145 centimeter-scale tephra layers at ~10%; similar estimates have been made by others

146 (Bonadonna et al. 2015). However, the estimated error varies according to tephra

147 thickness and it is difficult to quantify this uncertainty for historical measurements made

148 by several different people under varying conditions. Given the relatively small

149 observational error described in the literature, we have assumed that the historical

150 measurements in the literature are accurate to the nearest mm for the purposes of this

151 study.

152

153 Interpolation of initial tephra thickness

154 Ideally, the location of our measurements would have *exactly* replicated those used in

155 the original surveys, as recent research has demonstrated that tephra layers can be

156 highly variable over small spatial scales (Cutler et al. 2016b). Unfortunately, this was not

157 possible for the following reasons:

158   a) The original survey locations were not permanently marked. We had

159   coordinates for the MSH1980 sample points, but not H1947.

160   b) Many of the original measurements came from substrates that do not preserve

161   tephra layers (e.g., road surfaces, the roofs of cars and buildings, etc.)

162   c) Some of the original locations no longer exist (including measurements made

163   on ships that passed under the H1947 eruption plume, or sites subsequently

164   destroyed by anthropogenic activity and/or geomorphological processes).

165   d) Some deposits occurred on heavily managed landscapes, including ploughed

166   fields (eastern Washington State), and field systems dedicated to

167   grazing/fodder production where tephra was removed manually (southern

168   Iceland).

169 Terrestrial tephra layers are prone to disturbance, and these kinds of problems will face

170 any researcher seeking to compare extant tephra layers with measurements made

171 shortly after the eruption.

172

173 Given the near impossibility of replicating survey locations exactly, we had to take

174 measurements as close as possible to the original coordinates and use interpolation

175 techniques to estimate initial deposit thicknesses in our sample locations (due to the

176 relative sparsity of mass loading data, we decided not to interpolate this property). Many

177 previous studies have attempted to interpolate tephra thickness from a few points,

178 usually during the drafting of isopach maps. Our goal was slightly different: we wanted

179 to interpolate initial tephra thickness (with known variance) at arbitrary locations

180 downwind from the eruption. This goal meant we were not concerned with many of the

181 issues that have preoccupied previous researchers, such as calculating the total volume

182 of the deposit or inferring the edge of the fallout zone (Burden et al. 2013; Engwell et al.

183 2015; Yang and Bursik 2016).

184

185 Initial tephra thicknesses in our sampling locations were estimated from contemporary

186 records using the method developed by Yang & Bursik (2016). Briefly, this statistical

187 approach assumes that tephra thickness at an arbitrary location comprises: 1) a trend

188 component and 2) a random local component. Hence, when the data are log-

189 transformed, tephra thickness may be expressed as:

190

191 $$Th(s) = T(s) + Res(s) \text{ [eqn 1]}$$

192

193 where $Th(s)$ is the thickness at location s, $T(s)$ is the trend thickness and $Res(s)$ the local,

194 or residual, variation. The only data required to interpolate deposit thickness in the

195 model are a) the dominant wind direction during the eruption and b) some known values

196 of tephra thickness (in this case, the original values).

197

198   The trend component is largely a function of distance from the source vent and the

199   prevailing wind at the time of the eruption (which is assumed to be stable in strength

200   and direction). The local component is the result of numerous, small-scale processes

201   (e.g., turbulence structures in the plume) and is assumed to be spatially stochastic.

202   Yang and Bursik's (2016) approach models the two components separately and can

203   therefore accommodate phenomena such as the secondary thickening of the MSH1980

204   deposit observed by Sarna-Wojcicki *et al.* (1981). Following Yang and Bursik (2016), we

205   modelled the trend component using standard regression techniques, using radial

206   distance ($R(s)$) and downwind distance ($Dd(s)$) as explanatory variables (Online

207   Resource 2).

208

209   The local component was modelled using ordinary kriging on the residuals from the

210   multiple regression model. Kriging is an established interpolation technique that

211   provides a minimum variance estimate of a value at unmeasured locations, using a

212   model of autocorrelation structure (the theoretical variogram). Detailed descriptions of

213   kriging are available elsewhere (e.g., Isaaks and Srivastava 1989). Briefly, we produced

214   sample variograms from the residuals of the linear (trend) model. The sample

215   variograms described the relationship between semi-variance (a measure of

216   autocorrelation) in $\log_{10}(Th)$ and the distance between sampled locations. The sample

217   variograms were fitted with commonly used mathematical models by a process of trial-

218   and-error, using the 'gstat' package running in R (Pebesma 2004). We fitted spherical,

219   exponential and Gaussian models and selected the best fit by means of visual

220   inspection and a comparison of the weighted sum of squared errors for each model

221   (Bivand et al. 2013). The theoretical variogram that resulted was used during kriging,

222   carried out using the 'gstat' package after checking the residuals for normality.

223

224   Yang and Bursik's (2016) approach necessarily presents a much-simplified version of

225   reality: it is unable to accommodate factors such as changes in wind direction or

226   eruption dynamics, and complex processes in the atmosphere are reduced to simple

227   distance relationships. However, it does provide a robust, pragmatic and conceptually

228   straightforward method of inferring parameters such as tephra thickness at unmeasured

229   locations. It is particularly useful when details of eruption parameters are unavailable.

230

231   Field sampling of extant tephra layers

232

233   MSH1980

234   We conducted our surveys in the Gifford Pinchot National Forest (GPNF), 15 – 50 km

235   from Mt St Helens (hereafter, proximal locations), and at distal locations close to

236   Ritzville, WA (approx. 300 km from the eruption source: Fig. 2) in August 2015. We

237   chose sampling locations where the initial deposit thickness was moderate (~5 - 10 cm),

238   i.e., places where the tephra-fall would not have obliterated vegetation. The two

239   sampling areas have different climates: the GPNF has a moist, temperate climate; in

240   contrast, the Ritzville location has an arid, continental climate and frequently

241   experiences high winds (Online Resource 3). The vegetation cover in the two locations

242   also varies. The proximal location (~15 – 50 km from the vent) was characterized by

243   closed coniferous forest, composed primarily of hemlock (*Tsuga* sp.) and Douglas fir

244   (*Pseudotsuga menziesii*) (Fig. 4a). We surveyed old growth forest sites where the trees

245   on the sampling locations would have been mature at the time of the 1980 eruption. The

246   distal location was characterized by shrub/grassland dominated by sagebrush

247   (*Artemisia* sp.), a vegetation type known as sagebrush steppe (Fig. 4b). The sagebrush

248   locations we sampled had patchy vegetation cover: the areas between sagebrush/grass

249   patches often lacked vascular plants. Instead, these apparently bare areas were

250   covered by a thin (< 2.5 cm) biological soil crust (biocrust) composed of mosses, lichens

251   and, presumably, microorganisms such as fungi and cyanobacteria (Johansen 1993).

252

253   In the GPNF, we surveyed tephra layers along two transects established in 1980

254   (designated B-B' and C-C' in Waitt & Dzurisin (1981): see Fig. 2b). The transects ran

255   approximately north-south, perpendicular to the main axis of the 18 May eruption plume.

256   We surveyed 20 locations in total. The mean separation distance between our locations

257   and the original samples was 1.5 ± 0.4 km, with the majority of locations (10 of the 18

258   we used in our analysis) < 1 km from the 1980 survey locations. We recorded a) total

259   tephra layer thickness; b) the thickness of each unit within the tephra layer (where it was

260   possible to distinguish such features) following the nomenclature outlined in Waitt and

261   Dzurisin (1981) (refer to Online Resource 1 for details); c) the characteristics of the

262   understory vegetation cover and d) the thickness of soil/litter cover. We also collected

263   tephra samples from nine locations (refer to Online Resource 4). We used loss on

264   ignition (LOI) analysis to establish the proportion of organic material in the tephra layer.

265   The samples were homogenized before removing representative sub-samples. The

266   sub-samples were dried at 105 °C for a minimum of eight hours, then heated to 550 °C

267   for four hours to drive off organic material.

268

269   In the sagebrush steppe vegetation around Ritzville, we identified seven sampling

270   locations on an east-west transect (Fig. 2c). The survey of tephra layer thickness was

271   similar to that implemented in the GPNF (Online Resource 4). We collected a tephra

272   sample from one of the sampling locations, using the same methods deployed in the

273   GPNF, and backfilled the excavations.

274

275   H1947

276   We carried out surveys of the H1947 layer in southern Iceland in August 2017. We

277   targeted areas that were a) close to Thorarinsson's original (1954) sampling points

278   (mean separation distance 0.3 ± 0.1 km) and b) in the zone where the original tephra

279   deposit was of moderate thickness (< 10 cm). The region has a cold, moist maritime

280   climate and experiences frequent frosts (Online Resource 3). Our sampling locations

281   varied in character and the original points were imprecisely located, so we applied case-

282   by-case reasoning to locate suitable survey areas (refer to Online Resource 4 for details

283   of our approach). We sampled 12 locations in total.

284

285

286   **Results**

287

288   Interpolation of original tephra thickness

289   Our analysis of the original thickness measurements showed that both layers exhibited

290   exponential thinning with distance. The most parsimonious trend models were linear in

291   all cases; as the linear models were effective for our purposes (i.e., interpolating tephra

292   thickness 10s of km from the vent) we did not explore more complex non-linear models.

293   The introduction of breaks of slope can improve estimates of overall fallout volume,

294   because they capture variations in thickness close to the vent (Bonadonna and

295   Houghton 2005). However, this refinement was not relevant to our models, as the slope

296   for the whole deposit adequately captures the variation at the scale of interest. As the

297   plots of $\log_{10}$(thickness) vs absolute and downwind distance provided no compelling

298   evidence for introducing breaks in the trend models (Online Resource 5), we applied

299   multiple linear regression to model the trend in tephra thickness for both tephra layers.

300   The regressions were highly significant (MSH1980: $F_{2,160}$ = 116.2, p < 0.001; H1947:

301     $F_{2,59}$ = 45.7, p < 0.001), with adjusted R^2 values of ~0.6 in both cases.

302

303   The residuals of the trend models were approximately normal and therefore suitable for

304   ordinary kriging. The experimental variograms exhibited predictable increases in

305   semivariance with distance and we fitted spherical models to these variograms to

306   characterize local variations in tephra thickness (Online Resources 6, 7).

307

308   Field surveys

309   The MSH1980 tephra layer was found in all the sampling locations we visited in the

310   GPNF and in many cases the deposits could be divided into distinct stratigraphic sub-

311   units based on grain size and/or colour. The tephra layers were close to the surface:

312   most were covered by a thin (1 – 5 cm) layer of organic material (Figs 5, 6a). The

313   contacts between the tephra and the layers above and below were generally sharp. In

314   many sections, decayed timber (presumably from the 1980 forest floor) was clearly

315   visible at the base of the tephra deposit. Based on visual inspection, the stratigraphies

316   within each of the sample layers were consistent with the descriptions in Waitt &

317   Dzurisin's (1981) study. Within-site variability, expressed as a coefficient of variation

318   (CV; i.e., the sample standard deviation at each sampling location divided by the

319   sample mean) ranged from 0 – 33%, with most locations having a CV between 10 and

320   25% (Table 2). There was a thick layer of re-worked tephra in GP03 and this data point

321   was omitted from our analysis. Stratigraphic Unit B was missing (or not spotted) in

322   GP04. LOI analysis indicated that the tephra samples from the GPNF contained an

323   appreciable quantity of organic material/moisture (mean = 10.8 ± 1%).

324

325   Tephra layers were also found in all of the locations we selected around Ritzville. In

326   undisturbed areas, the MSH1980 tephra layer was found just below a thin (3 – 25 mm)

327   biocrust. The layer was uniformly fine and pale grey (Fig. 6b). In most cases, both the

328   top and bottom surfaces of the layer were sharply defined. Within-site variability was

329   generally low: although a CV figure of 33% was observed at R06, the remaining six

330   locations had values below 16% (Table 2). LOI analysis of a single sample from the

331   Ritzville area indicated that the proportion of organic material/moisture was 7.7%.

332

333   Areas with an intact H1947 layer were hard to locate. We eventually identified 12

334   locations that satisfied our criteria (Fig. 3, Table 2). All but one of the sampling locations

335   was within 500 m of Thorarinsson's (assumed) original measurement; the greatest

336   separation distance was 1.16 km. The H1947 layer was more variable than MSH1980 in

337   terms of thickness: the CV figures ranged from 21-65%, with most of our sampling

338   locations displaying a CV around 30% (Table 2). The layer was also buried more

339   deeply, with ~4 – 10 cm of overlying sediment (Fig. 6c), and appeared to be unstratified.

340   LOI analysis indicated that the H1947 tephra samples had consistently low organic

341   content (0.4 – 3.9%; mean = 2.3 ± 0.4%).

342

343   [Table 2: Summary of tephra measurements]

344   [Fig. 5: MSH1980 stratigraphy]

345

346   Tephra layer thickness and mass loading

347   In the GPNF, tephra thickness varied predictably along transect C-C', i.e., the values

348   were lowest toward the margins of the fallout zone (where the layer became

349   increasingly patchy) and thickest towards the axis of the eruption plume (Fig. 5). The

350   layer was thicker along transect B-B', but did not exhibit a systematic thickening towards

351   the axis of the fallout zone. Mass loadings for the GPNF sampling locations ranged from

352   1.6-10.3 g cm^{-2} (Fig. 7). The highest mass loading was recorded close to the main axis

353   of the eruption plume (i.e., where Waitt & Dzurisin's transect AA' intersects CC': Fig.

354   7b). Mass loadings decreased with distance from the plume axis. There was no

355   systematic variation in layer thickness along the east-west transect line established

356   outside Ritzville (within an area of secondary thickening). The tephra sample taken from

357   this location had a mass loading of 2.3 g cm^{-2} (Fig. 7a).

358

359   [Fig. 6: Field images of tephra layers]

360   [Fig. 7: MSH mass loadings]

361

362   The thickness and mass loading of the H1947 layer did not vary predictably with

363   distance from the vent and main axis of the plume. The most distal sampling location

364   (Hk12) had the thinnest tephra layer (1.5 cm). However, the layer was a similar

365   thickness (1.9 cm) at the most proximal sampling location (Hk01) (Table 2). The

366   sampling location with the thickest layer (Hk08: 5.9 cm) was an intermediate distance

367   from the vent, and away from the main axis of the plume. Most sampling locations had a

368   thickness of 2 -3 cm, regardless of location. The mass loading figures were similarly

369   unpredictable, with most sampling locations between $2 - 3$ g cm^{-2} (Table 2). Sampling

370   location Hk08 was an outlier: the mass loading here (4.2 g cm^{-2}) was the highest

371   recorded and twice that of adjacent locations.

372

373   [Fig. 8: Hekla mass loading results]

374

375   Comparison of findings with original measurements

376   Thickness measurements from the MSH1980 layer were positively correlated with

377   interpolated initial thicknesses (Fig. 9). However, there was a difference between the

378   GPNF and Ritzville samples. The Ritzville measurements were close to, or slightly

379   below, the interpolated values (Fig. 9a, blue points). The tephra layer here had a mean

380   thickness of 3.4 ± 0.2 cm. An initial thickness of 4.2 cm was recorded at a nearby

381 location in 1980 (IAVCEI 2010), i.e., the thickness of the preserved layer was around

382 80% of the initial deposit. In contrast, the layer in the GPNF appeared to be *thicker* than

383 the interpolated values (Fig. 9a, red points), in some cases by up to 200% (GP01). Our

384 measurements fell below the interpolated values on just two sampling locations.

385

386 The mass loading data from MSH1980 followed a similar pattern. Transect CC' (along

387 which we collected our GPNF mass loading samples) is about 32 km from MSH,

388 measured along the plume axis. Reading from a plot of mass loading vs distance in

389 Sarna-Wojcicki *et al.* (1981: their figure 339), the estimated mass loading at the

390 intersection of the plume axis with CC' was 8 g cm^{-2}. We recorded a figure of 10.3 g cm^{-2}

391 for approximately the same location (i.e., slightly higher than the original figure). The

392 samples from Ritzville told a similar story. The isomass map in Sarna-Wojcicki *et al.*

393 (their figure 338) suggests mass loadings between 2.0 and 2.5 g cm^{-2} around Ritzville.

394 Our recorded value of 2.3 g cm^{-2} fitted neatly in this range.

395

396 The correlation between initial and preserved thickness was much weaker for the

397 H1947 layer (Fig. 9b). The measured thicknesses were consistently lower than the

398 interpolated initial values (10 of the 12 sampling locations). In many cases, the

399 preserved layer was >50% thinner than the initial deposit. The pattern of the mass

400 loading values was similar: most were much lower than those observed in 1947 (Fig. 8).

401 Two locations departed from this: the mass loading at Hk08 was similar to the initial

402 value; the value recorded for Hk05 (2.7 g cm^{-2}) greatly exceeded Thorarinsson's

403 measurement (0.9 g cm^{-2}).

404

405   [Fig. 9: Comparison of measured and interpolated values]

406

407

408   **Discussion**

409   The preservation of the tephra layers varied both within and between the two eruptions.

410   Preservation of the MSH1980 layer in areas of light anthropogenic disturbance was

411   good. Broad trends in thickness and mass loading apparent in the initial deposit were

412   retained in the tephra layer (i.e., both metrics decreased with distance from the vent and

413   the main axis of the plume). This was particularly clear on transect C-C' (the sampling

414   locations on B-B' were probably too close to the plume axis to show a marked pattern).

415   Small-scale stratigraphy was also preserved (GPNF sampling location) and within-site

416   variability was low: small- (metre-) scale factors had not obscured the volcanic signal.

417   The same could not be said of the H1947 layer, which exhibited considerable variability

418   at all scales and disrupted stratigraphy.

419

420   We anticipated that the tephra layers would undergo a degree of post-depositional

421   transformation, particularly the H1947 layer (deposited on a snow-covered, managed

422   landscape). A degree of bioturbation would be expected in moist, productive habitats

423   like the GPNF (Blong et al. 2017). Even if no tephra were lost through the action of wind

424   and water, thinning due to compaction is likely. Very little research has been conducted

425   on the rate/magnitude of tephra compaction. Some researchers have applied 'rule of

426   thumb' adjustments to allow for compaction: for example, Sarna-Wojcicki *et al.* (1981)

427 increased their estimate of initial layer thickness in the Ritzville area by a factor of two

428 after a rainfall event, based on mass loading figures. Placing constraints on the rate of

429 tephra compaction, either by direct measurement of fresh deposits, or experimental

430 manipulation, would clearly be a useful goal for future research.

431

432 Given these factors, the level of preservation we observed in the MSH1980 layer was

433 unexpected. Our surveys revealed little or no evidence of bioturbation. We did not find

434 litter in the samples during collection, average organic content (in the form of fine roots,

435 soil organic matter (SOM) and soil microbes) was comparatively low and contacts with

436 the surrounding soil were usually sharp. These observations are consistent with limited

437 mixing, and, whilst it is probable that some tephra grains have been lost to other soil

438 horizons, the thickness and mass loading figures suggest such losses were limited.

439 Major re-working of the layer by slope processes was only observed in one sampling

440 location in the GPNF (GP03, subsequently omitted from our analysis).

441

442 Our previous work in Iceland suggests that biophysical feedbacks, specifically

443 vegetation structure (and its likely impact on surface wind conditions), plays an

444 important role in tephra retention (Cutler et al. 2016a; Cutler et al. 2016b; Dugmore et

445 al. 2018). Closed forest (such as that found in the GPNF) should, in principle, be a good

446 environment for the stabilization of tephra, because the forest canopy reduces surface

447 wind speed (Online Resource 3) and intercepts a significant proportion of the

448 precipitation. The degree of ground disturbance by large herbivores is also limited,

449 when compared to pasture land. The coniferous forests of the Pacific North West are

450 highly productive, and the rapid accumulation of an organic layer on top of the tephra

451 could assist in preservation, as could the formation/persistence of a thick ground layer

452 of vegetation.

453

454 Even allowing for favourable conditions, the fact that most of the GPNF measurements

455 exceeded the interpolated initial thicknesses is a puzzle. The apparent discrepancy

456 could be due to the input of allochthonous (non-volcanogenic) sediment post-deposition.

457 We assumed that the inorganic component of the samples was mainly tephra, but it is

458 possible that a small component of fine, non-volcanogenic sediment (i.e., produced by

459 rock weathering) may have been included (particularly in the samples from the semi-

460 arid sagebrush steppe), compensating for losses of tephra. However, the fine-scale

461 stratigraphy of the layers suggests that additions of this type were limited. Uncertainty in

462 the interpolation process might have also contributed towards the seemingly anomalous

463 result. The trend model included unexplained variance; furthermore, we were not able to

464 replicate the original sampling locations and kriging variance increases with distance

465 from the points used to generate the sample variogram (Bivand et al. 2013). However,

466 we believe the pattern observed in the GPNF was real because:

467   a) It was persistent (all but one of our measurements exceeded the interpolated

468   values, sometimes by a factor of two);

469   b) The trend model was effective in explaining variance in tephra depth; local

470   variance made a relatively minor contribution to tephra thickness (typically < 20%

471   in the case of the GPNF measurements);

472   c) None of our GPNF sampling locations were more than 7.4 km from a USGS

473   survey location (typically much closer), so the kriging variance was low (Online

474   Resource 7);

475   d) Where our sampling locations were close to the 1980 sites (< 1 km separation, in

476   some instances) the pattern was preserved (i.e., it is unlikely to be an artefact of

477   the interpolation).

478 In addition, the mass loading figure for GP16, close to the main axis of the plume,

479 exceeded the value estimated Sarna-Wojcicki *et al.*'s (1981) survey.

480

481 If the tephra layer in the GPNF is, indeed, thicker and heavier than the deposit

482 measured shortly after the eruption, this suggests a) rapid and near-complete

483 stabilization of the tephra, with little compaction and b) the addition of further tephra

484 after first measurements were made. Further tephra may have been added to the 1980

485 layer after the 18 May eruption, as there were subsequent tephra-producing eruptions.

486 The plume from one of these eruptions (22 July) was blown eastwards and may have

487 added a few millimetres of tephra to the 18 May deposit (Waitt et al. 1981).

488 Furthermore, it is possible that tephra from the 18 May eruption was deposited *after*

489 measurement. Zobel and Antos (1991) noted that coniferous trees trapped tephra

490 during the initial air-fall event, and that this material reached the ground sometime after

491 the eruption. Measurement techniques may also account for some apparent

492 discrepancies. Sarna-Wojcicki *et al.* (1981) noted that other observers reported greater

493 thicknesses of tephra, but suggested that these reports were due to earlier observations

494 (i.e., they were made before compaction had occurred) or the reporting of maximum,

495   rather than average, thicknesses. The incorporation of organic material (typically around

496   11% by mass in GPNF) may also have enhanced the thickness of the layer. Whatever

497   the reasons, it seems that preservation of the tephra layer under close coniferous forest

498   has been unusually good.

499

500   We observed very little site-to-site variation in the thickness of the distal MSH1980

501   layer. This was unsurprising as the sampling locations lie parallel with the main axis of

502   the plume in a region where the rate of change in thickness with distance was low. As in

503   the GPNF, the degree of tephra retention on undisturbed land around Ritzville was

504   remarkable, particularly given how susceptible this fine-grained material must have

505   been to erosion by wind (Online Resource 3). In order to retain so much fine material,

506   stabilization of the tephra must have been rapid, particularly as the patchy vegetation of

507   the sagebrush steppe would seem to be a much less favourable environment for

508   preservation than the closed canopy forest. The retention of the tephra layer in open

509   areas (i.e. between sagebrush/grass patches) was particularly surprising, as the ground

510   surface was relatively smooth and exposed to the elements. The lack of variation in

511   tephra thickness between vegetated and non-vegetated areas around Ritzville was also

512   unexpected. In Iceland, the thickness of tephra layers is positively correlated with

513   vegetation height/density (Cutler et al. 2016a), so we expected that the layer would be

514   thicker under sagebrush clumps.

515

516   The lack of variation in the Ritzville locations implies that the mechanisms for stabilizing

517   tephra in open areas were just as effective as those operating beneath vegetation.

518   Again, it is possible that biophysical processes have influenced tephra preservation: we

519   suspect that the stabilization of tephra in open areas was due to biocrust formation. A

520   thin crust was present in all the locations we sampled and was clearly capable of

521   capping-off the underlying deposit. Cyanobacteria can colonize suitable substrates in a

522   matter of days to initiate biocrust formation. Thereafter, biological succession can occur,

523   with increasing cover of bryophytes and lichens being particularly important. Rozenstein

524   *et al.* (2014) note that in certain conditions a biocrust can form within weeks, and that

525   biocrust formation on fine substrates is much faster, and more homogeneous, than it is

526   on coarse grains. An investigation of the biocrust composition and rate of formation

527   would be a useful focus of future study.

528

529   In contrast to the MSH1980 layer, preservation of the H1947 layer was spatially

530   variable, even in areas where presumed human interference was low. The mass loading

531   observed at Hk08, which initially appeared to be an outlier, was actually closest to the

532   1947 value. This area differs from the other sampling locations, in that it sits in the

533   bottom of a shallow, semi-enclosed basin. It is therefore possible that tephra re-

534   mobilized from adjacent, unvegetated slopes supplemented the initial deposit. Most

535   other sampling locations had experienced losses of tephra, but one (Hk05) appeared to

536   have gained material. Southern Iceland is a wet and windy locality (Online Resource 3)

537   subject to significant cryoturbation (evidenced by patterned ground and frost hummocks

538   (*thufur*), on our field sites). Vegetation is low-growing and often sparse. However, we

539   know that tephra from recent eruptions in southern Iceland has been extensively

540   mobilized in the months following the eruption, even when the eruption was in spring

541   (Arnalds et al. 2013). Similar remobilization has been observed following other

542   eruptions, both in Iceland (Liu et al. 2014) and South America (Panebianco et al. 2017;

543   Wilson et al. 2011). During the 1947 eruption, the surface vegetation would have been

544   suffering from winter dieback. It is therefore likely that a significant proportion of the

545   initial H1947 deposit was re-mobilized after its initial deposition. Fine-scale variation in

546   surface roughness would have led to the local differences in tephra thickness and mass

547   loading that we observed. For example, on Hk11 we noted that the H1947 layer was

548   absent from the 'crests' of small hummocks. Furthermore, the tephra fell during winter

549   when there was patchy snow cover and extensive ground ice formation. Tephra falling

550   on snow patches would have been re-worked when the snow melted. Any remaining

551   stratigraphy would have been disrupted by the formation of ground (needle) ice.

552   Geomorphological processes have clearly been important in the preservation of the

553   H1947 layer. In this setting, accurate reconstruction of the fallout from the preserved

554   layer would be extremely challenging. Had the tephra fallen on equivalent vegetation in

555   a less geomorphologically active setting, the preservation of the layer might have been

556   much better.

557

558   Tephrostratigraphy relies on the use of isochronous layers, which, ideally, represent

559   only the primary fallout. However, we suspect that terrestrial tephra deposits are

560   routinely transformed by processes operating over a range of (frequently overlapping)

561   timescales. The operation of these processes may make it hard to separate unmodified

562   and transformed deposits reliably. When tephra is exposed at the surface, it is subject

563   to both erosion and the stabilizing effect of vegetation. Compaction and disruption by ice

564 growth and decay can occur both above and below ground. Once interred, it is affected

565 by both biological and abiotic processes such as root growth, bioturbation, through-flow

566 and solifluction. Some transformations, such as those resulting from earthquakes and

567 land sliding, may occur through the full depth of the soil/regolith. We do not know the

568 duration of the processes that physically transform tephra layers; they may operate for

569 as long as the tephra layer exists. We suspect that the rate of change is highest just

570 after deposition and decreases with time as the tephra layer is progressively buried.

571 Transformation of the tephra may be continuous or episodic; the rate of change may

572 alter abruptly as different factors come into play (e.g., the rate of transformation could

573 reduce sharply on first burial as the tephra is no longer affected by surface processes).

574 We suspect that the genesis of terrestrial tephra layers varies on a site-by-site basis

575 according to climate, vegetation cover, topographic location, time and the properties of

576 both the soil/regolith and the tephra layer itself. However, the trajectory of change can

577 only be established by longitudinal studies. Regardless of how the transformation

578 proceeds, it appears that terrestrial tephra deposits can undergo modification without

579 showing obvious signs of re-working (e.g., diffuse contacts with the soil, disrupted

580 stratigraphy, etc.) and this process can operate without markedly increasing spatial

581 patchiness (i.e., all of the deposit in a given area can be transformed in the same way).

582 Indeed, our experience with the H1947 layer suggests that tephra layers can become

583 more spatially homogeneous over time. Hence, terrestrial tephra layers have to be

584 carefully assessed for transformations before they are used to infer volcanological

585 parameters and processes.

586

587

Conclusions

589 We hypothesized that the MSH1980 and H1947 tephra layers would capture the overall

590 characteristics of the fallout that created them (i.e., systematic thinning and reduction in

591 mass loading). However, we expected the transformation of both their physical

592 properties and internal structure (H1). We also anticipated that vegetation cover would

593 mediate this transformation, e.g., the degree of preservation of the MSH1980 layer in

594 GPNF would be higher than that in the sagebrush steppe (H2). We found that the

595 MSH1980 tephra layer captured the overall characteristics of the original deposit.

596 However, the degree of preservation varied markedly between Washington State and

597 Iceland – the MSH1980 layer had a higher level of preservation - and the layers did *not*

598 thin predictably during preservation. It was difficult to calibrate the preservation of the

599 MSH1980 layer in the GPNF, because there is strong evidence that contemporary

600 measurements underestimated the original deposit. If the original measurements had

601 captured the whole deposit, we may well have seen the thinning/mass loss we

602 anticipated. In Iceland, the H1947 layer did not retain the overall characteristics of the

603 initial deposit, due to the operation of local-scale biophysical feedbacks which resulted

604 in variable preservation. The collection of more samples, spread over a wider area,

605 might have given a clearer picture, but it was clear that the signal from the initial deposit

606 was largely scrambled. Hence, the support for our first hypothesis was qualified, at best.

607

608 It appeared that vegetation cover played a role in tephra preservation. The Icelandic

609 sampling locations, characterized by low-growing and sometimes sparse vegetation,

610 had variable (often poor) preservation. In contrast, the closed tree cover of the GPNF

611 was associated with a high level of tephra preservation. However, against expectations,

612 we also found good preservation in the sparse vegetation of the sagebrush steppe,

613 hinting at the previously unsuspected significance of biocrusts (a cover type

614 characteristic of ~70% by area of global drylands: Ferrenberg et al. 2015). Hence, whilst

615 we found evidence consistent with H2, we also revealed a more nuanced relationship

616 between ground cover, geomorphological processes and tephra preservation. These

617 findings reinforce our belief that reconstructions of past eruption histories based on

618 terrestrial tephra records are sensitive to surface conditions (specifically vegetation

619 cover) at the time of the eruption. Hence, inferred volcanological parameters based on

620 these deposits should be treated with due caution. The effect of surface conditions on

621 tephra preservation (and, by extension, volcanological inferences) will be particularly

622 marked when a tephra deposit crosses regions of contrasting vegetation cover.

623

624

28

633

634

635 **References**

636

637 Arnalds O, Thorarinsdottir EF, Thorsson J, Dagsson Waldhauserova P, Agustsdottir AM

638 (2013) An extreme wind erosion event of the fresh Eyjafjallajokull 2010 volcanic ash. Sci

639 Rep-UK 3

640 Bivand RS, Prebesma E, Gómez-Rubio V (2013) Applied spatial data analysis with R.

641 Springer, New York

642 Blong R, Enright N, Grasso P (2017) Preservation of thin tephra. Journal of Applied

643 Volcanology 6. https://doi.org/10.1186/s13617-017-0059-4

644 Bonadonna C, Biass S, Costa A (2015) Physical characterization of explosive volcanic

645 eruptions based on tephra deposits: Propagation of uncertainties and sensitivity

646 analysis. Journal of Volcanology and Geothermal Research 296:80-100

647 Bonadonna C, Houghton BF (2005) Total grain-size distribution and volume of tephra-

648 fall deposits. B Volcanol 67:441-456

649 Burden RE, Chen L, Phillips JC (2013) A statistical method for determining the volume

650 of volcanic fall deposits. B Volcanol 75

651 Cutler NA, Bailey RM, Hickson KT, Streeter RT, Dugmore AJ (2016a) Vegetation

652 structure influences the retention of airfall tephra in a sub-Arctic landscape. Prog Phys

653 Geog 40:661-675

654   Cutler NA, Shears OM, Streeter RT, Dugmore AJ (2016b) Impact of small-scale

655   vegetation structure on tephra layer preservation. Sci Rep-UK 6.

656   https://doi.org/10.1038/srep37260

657   Dugmore A, Streeter R, Cutler N (2018) The role of vegetation cover and slope angle in

658   tephra layer preservation and implications for Quaternary tephrostratigraphy.

659   Palaeogeogr Palaeocl 489:105-116

660   Engwell SL, Aspinall WP, Sparks RSJ (2015) An objective method for the production of

661   isopach maps and implications for the estimation of tephra deposit volumes and their

662   uncertainties. B Volcanol 77. https://doi.org/10.1007/s00445-015-0942-y

663   Engwell SL, Sparks RSJ, Aspinall WP (2013) Quantifying uncertainties in the

664   measurement of tephra fall thickness. Journal of Applied Volcanology 2. 10.1186/2191-

665   5040-2-5

666   Ferrenberg S, Reed SC, Belnap J (2015) Climate change and physical disturbance

667   cause similar community shifts in biological soil crusts. PNAS 112:12116-12121

668   Houghton B, Carey RJ (2015) Pyroclastic fall deposits. In: Siggurdsson H, Houghton B,

669   McNutt SR, Rymer H, Stix J (eds) Encyclopdia of Volcanoes. Academic Press, London,

670   pp 599-616

671   IAVCEI (2010) Data sets. IAVCEI Commission on Tephra Hazard Modelling.

672   http://www.ct.ingv.it/iavcei/data/MSH/MSH80_location-thickness.txt. Accessed 25 April

673   2018

674   Isaaks EH, Srivastava RM (1989) An introduction to applied geostatistics. Oxford

675   University Press, New York

676   Johansen JR (1993) Cryptogamic crusts of semiarid and arid lands of North America. J

677   Phycol 29:140-147

678   Liu EJ, Cashman KV, Beckett FM, Witham CS, Leadbetter SJ, Hort MC, Guomundsson

679   S (2014) Ash mists and brown snow: Remobilization of volcanic ash from recent

680   Icelandic eruptions. Journal of Geophysical Research-Atmospheres 119:9463-9480

681   Lowe DJ (2011) Tephrochronology and its application: A review. Quat Geochronol

682   6:107-153

683   Panebianco JE, Mendez MJ, Buschiazzo DE, Bran D, Gaitan JJ (2017) Dynamics of

684   volcanic ash remobilisation by wind through the Patagonian steppe after the eruption of

685   Cordon Caulle, 2011. Sci Rep-UK 7

686   Pebesma EJ (2004) Multivariable geostatistics in S: the gstat package. Comput Geosci

687   30

688   Pyle DM (1989) The thickness, volume and grainsize of tephra fall deposits. B Volcanol

689   51:1-15

690   Pyle DM (2016) Field observations of tephra fallout. In: Mackie S, Cashman K, Ricketts

691   H, Rust A, Watson M (eds) Volcanic Ash. Elsevier, Amsterdam, pp 25-38

692   Rozenstein O, Zaady E, Katra I, Karnieli A, Adamowski J, Yizhaq H (2014) The effect of

693   sand grain size on the development of cyanobacterial biocrusts. Aeolian Res 15:217-

694   226

695   Sarna-Wojcicki AM, Shipley S, Waitt RB, Dzurisin D, Wood SH (1981) Areal distribution,

696   thickness, mass, volume, and grain size of air-fall ash from the six major eruptions in

697   1980. In: Lipman PW, Mullineaux DR (eds) The 1980 eruption of Mount St Helens,

698   Washington, U.S. U.S. Department of the Interior, USGS, Washington D.C., pp 577-600

699   Thorarinsson S (1954) The tephra fall from Hekla on March 29th 1947. Societas

700   Scientarium Islandica, Reykjavik

701   Waitt RB, Dzurisin D (1981) Proximal air-fall deposits from the May 18 eruption -

702   stratigraphy and field sedimentology. In: Lipman PW, Mullineaux DR (eds) The 1980

703   eruption of Mount St. Helens, Washington. US Department of the Interior, USGS,

704   Washington D.C., pp 601-616

705   Waitt RB, Hansen VL, Sarna-Wojcicki AM, Wood SH (1981) Proximal air-fall deposits of

706   eruptions between May 24 and August 7, 1980 - stratigraphy and field sedimentology.

707   In: Lipman PW, Mullineaux DR (eds) The 1980 eruption of Mount St. Helens,

708   Washington. U.S. Department of the Interior, USGS, Washington D.C., pp 617-628

709   Wilson TM, Cole JW, Stewart C, Cronin SJ, Johnston DM (2011) Ash storms: impacts of

710   wind-remobilised volcanic ash on rural communities and agriculture following the 1991

711   Hudson eruption, southern Patagonia, Chile. B Volcanol 73:223-239

712   Yang QY, Bursik M (2016) A new interpolation method to model thickness, isopachs,

713   extent, and volume of tephra fall deposits. B Volcanol 78.

714   https://doi.org/10.1007/s00445-016-1061-0

715   Zobel DB, Antos JA (1991) 1980 tephra from Mount St Helens - spatial and temporal

716   variation beneath forest canopies. Biol Fert Soils 12:60-66

717

718

719 **Table captions**

720

721 **Table 1** Characteristics of the MSH1980 and H1947 eruptions; the estimated fallout

722 area from MSH1980 is based on the area of the 1 mm isopach given in Engwell *et al.*

723 (2015)

724

725 **Table 2** Summary of survey data (T = thickness; CV = coefficient of variation in

726 thickness measurement; SE = standard error). Site codes: GP = Gifford Pinchot

727 National Forest; R = Ritzville; Hk = Hekla

Figure captions

Fig. 1 Conceptual diagram illustrating the post-depositional transformation of tephra

layers

Fig. 2 MSH1980 sampling locations; our sampling points are indicated by the numbered

red circles; the original sampling points are indicated with open circles and the isopachs

of 1980 fallout with orange lines; the State boundary is shown with a continuous black

line; a) location plan, showing the proximal (GPNF) and distal (Ritzville) sampling areas;

the location of Mount St Helens is indicated by a black triangle; b) detail of the GPNF

sample locations; the blue lines indicate transects established in the original survey of

the tephra deposit; black parallel lines indicate major roads; c) detail of the Ritzville

sample locations (the location of Ritzville is indicated by a black square). Isopachs and

sampling points from Sarna-Wojcicki *et al.* (1981); tephra thicknesses are in mm

Fig. 3 H1947 sampling locations (red circles), with the original sample locations

indicated by open circles; isopachs (orange lines) from Thorarinsson (1954);

settlements are indicated by black square; icecaps are outlined in black; tephra

thicknesses are in mm

Fig. 4 The three different environments that we surveyed; a) the closed coniferous

forest that characterizes the GPNF sample locations (for scale, the trees in the middle

750   ground are approximately 50 cm in diameter); b) sagebrush steppe around Ritzville; c)

751   heathland in southern Iceland (note the eroded slopes in the middle ground)

752

753   **Fig. 5** The average thickness of the MSH1980 layer in the GPNF (sampling location

754   reference numbers are given below each section). Data from our sampling locations

755   have been arranged along Waitt & Dzurisin's B-B' and C-C' section lines and the

756   designation of the tephra units follows their nomenclature (Waitt and Dzurisin 1981).

757   The position of section A-A' (which approximates the main axis of the plume) is shown

758   in each case

759

760   **Fig. 6** Representative images of the tephra layers showing a) the MSH1980 layer in the

761   GPNF; b) the MSH1980 layer at a distal location outside Ritzville and c) the H1947

762   layer. Note the more recent Eyjafjalajökull 2010 tephra layer above the H1947 deposit,

763   and the older Katla 1918 layer below

764

765   **Fig. 7** MSH1980 mass loading data; a) Waitt and Dzurisin's (1981) mass loading data,

766   showing their isomass lines (blue, with mass in g cm^{-2}) and our sampling locations (red

767   circles); our observed mass loading for the Ritzille area is in bold red text; b) our mass

768   loading figures for the GPNF sampling locations (in g cm^{-2}), compared to the isomass

769   lines from the original survey; Waitt and Dzurisin's transect lines are shown for

770   reference; c) our mass loading figures arranged along Waitt and Dzurisin's (1981)

771   transect C-C' in the GPNF; the red vertical line indicates the intersection with transect

772   A-A', which coincides with the plume axis

773

774 **Fig. 8** H1947 mass loading data; Thorarinsson's (1954) original measurements are

775 shown as green circles, scaled according to his measurements (the green figures in g

776 cm^{-2}); our measurements represented by red circles on the same scale (the red figures,

777 also in g cm^{-2}); the orange line indicates Thorarinsson's 1 mm isopach line; open circles

778 indicate Thorarinsson's original sampling points and black squares settlements; icecaps

779 are outlined in black

780

781 **Fig. 9** Comparison of measured and interpolated values from MSH1980 (top) and

782 H1947 (bottom)

783
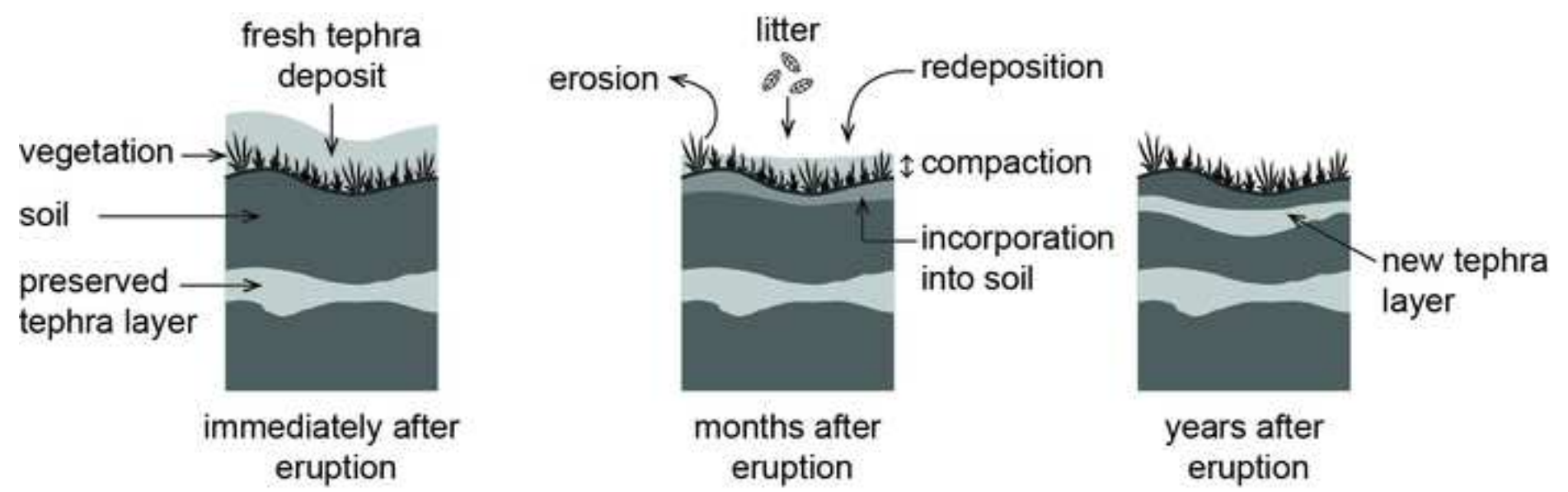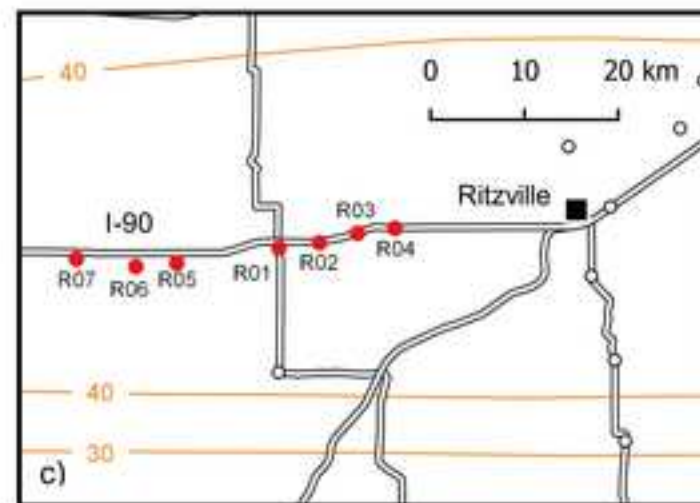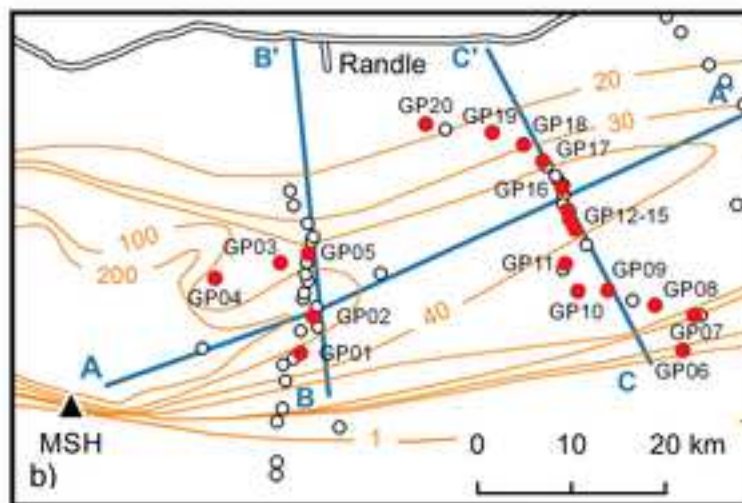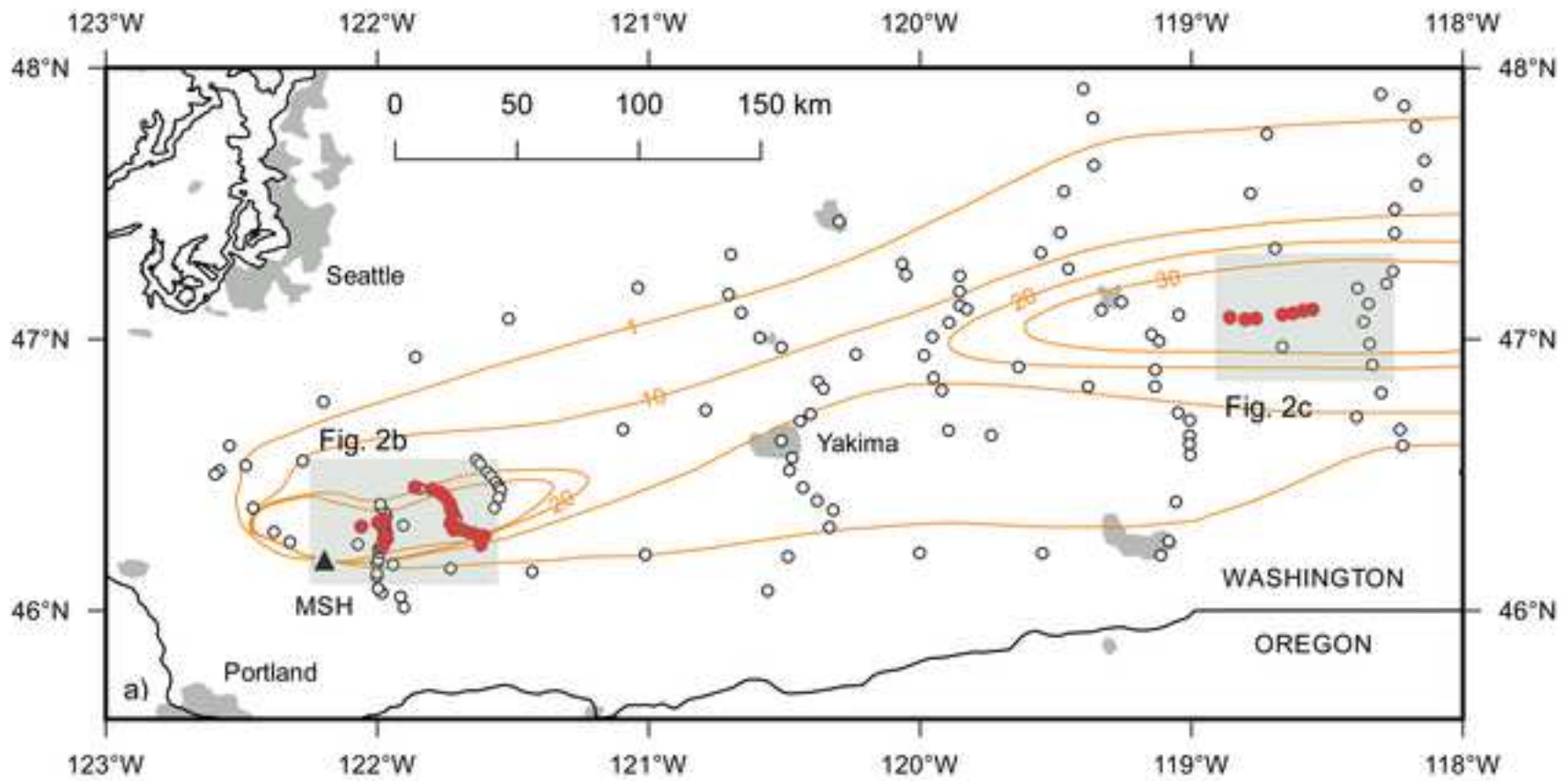
Figure 1

Figure 2

Figure 3

Click here to access/download;Figure;Fig. 3_H1947_map.jpg ⬇

Figure 4

MSH1980

H1947

Section B-B'

A-A'

KEY

0

10

20

30

40 cm

GP01

GP02

GP04

GP05

soil cover

unit C

tephra layer

unit B

unit A

1980 substrate

Section C-C'

A-A'

GP06

GP08

GP09

GP10

GP11

GP12

GP13

GP14 GP15

GP16

GP17

GP18

GP19

unassigned unit

0   1   2   3   4   5 km
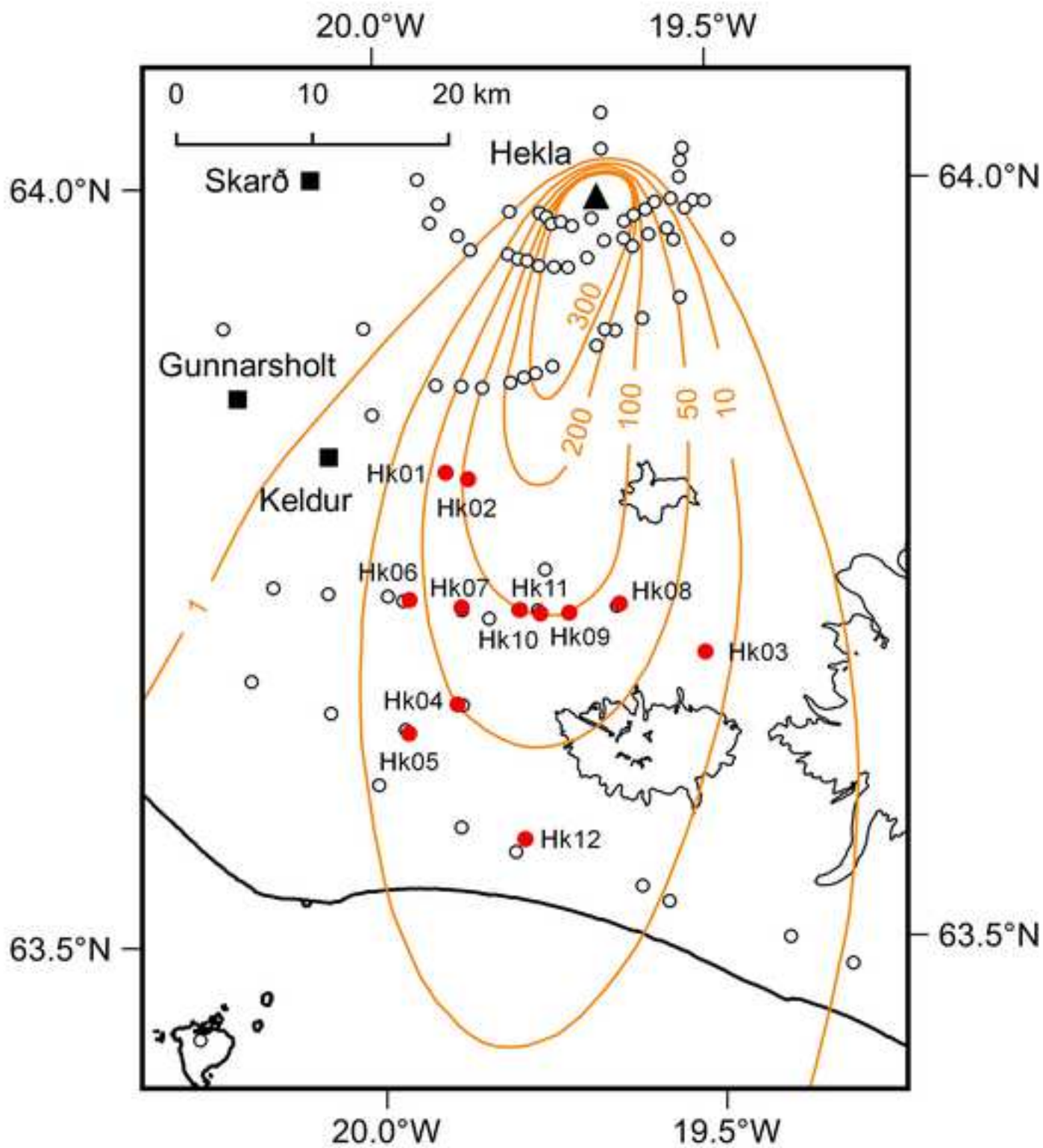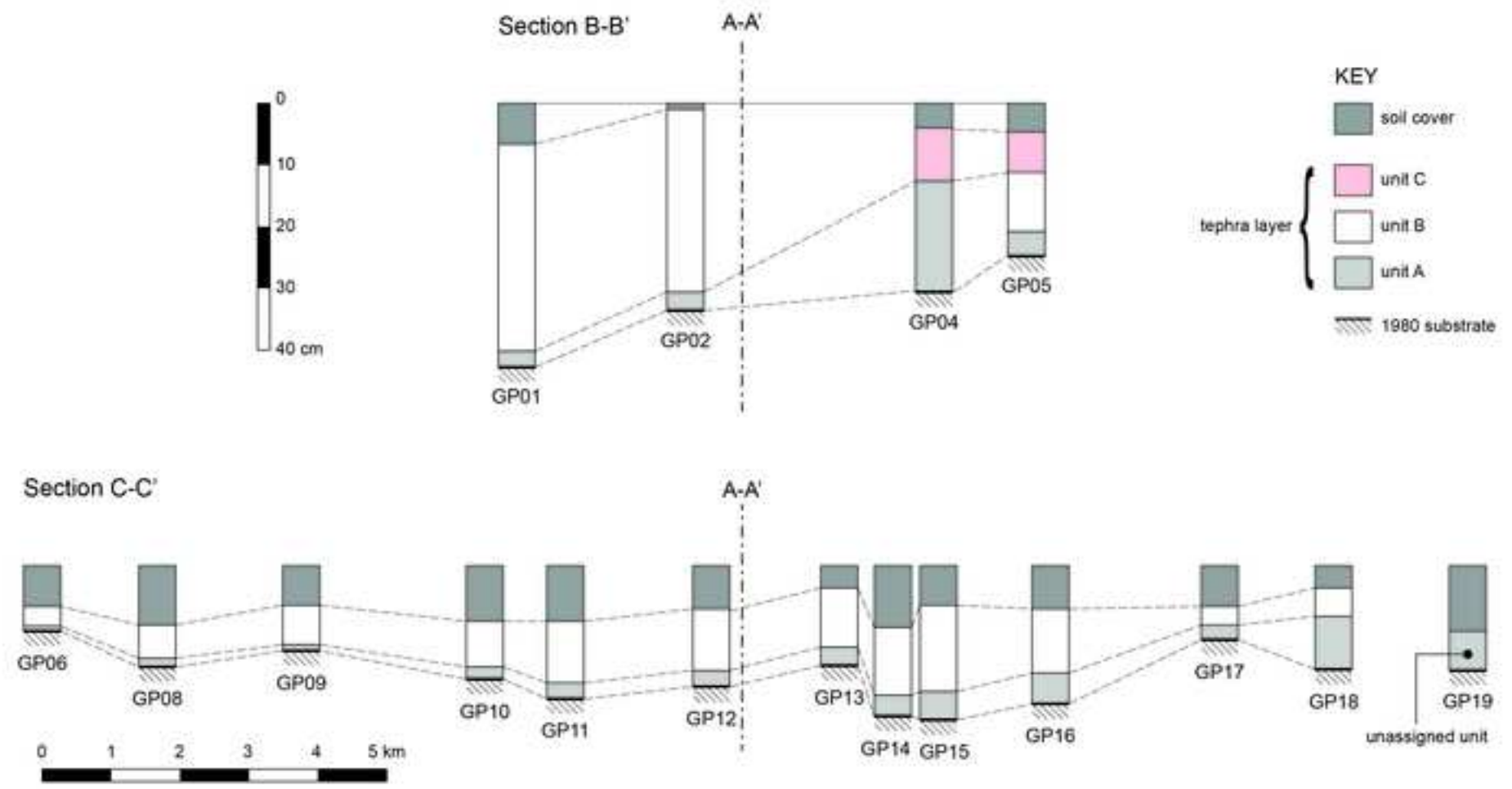
Figure 7

Click here to access/download;Figure;Fig. 7_MSH_ML_rev1.jpg
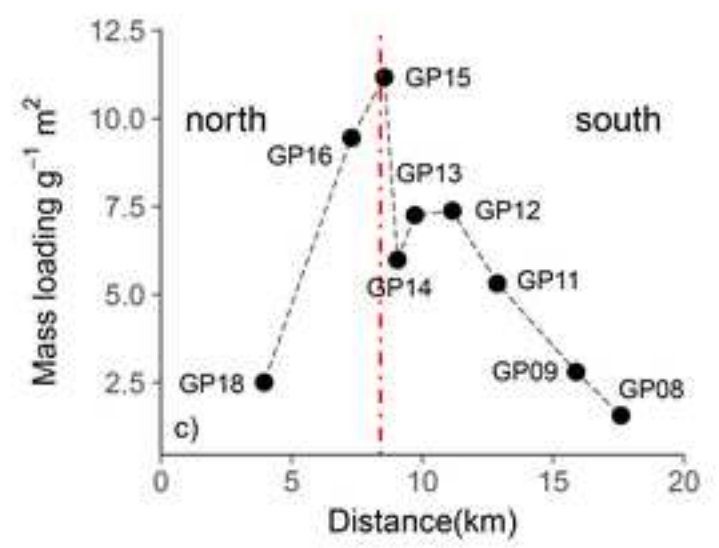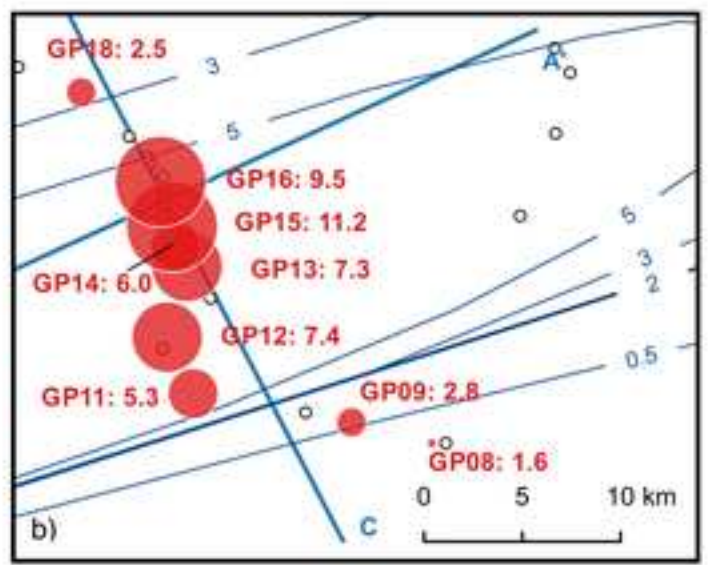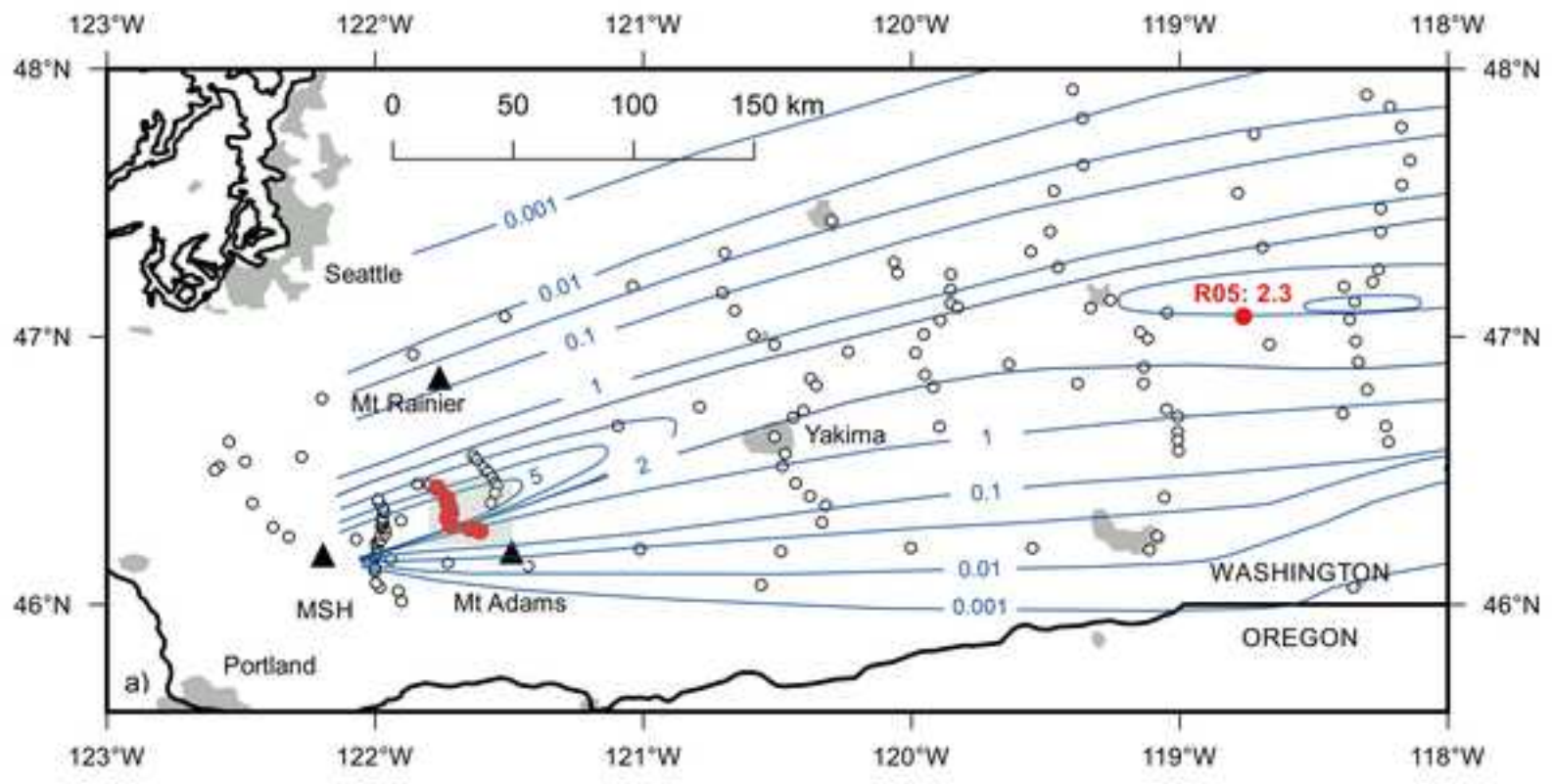
Figure 8

Figure 9
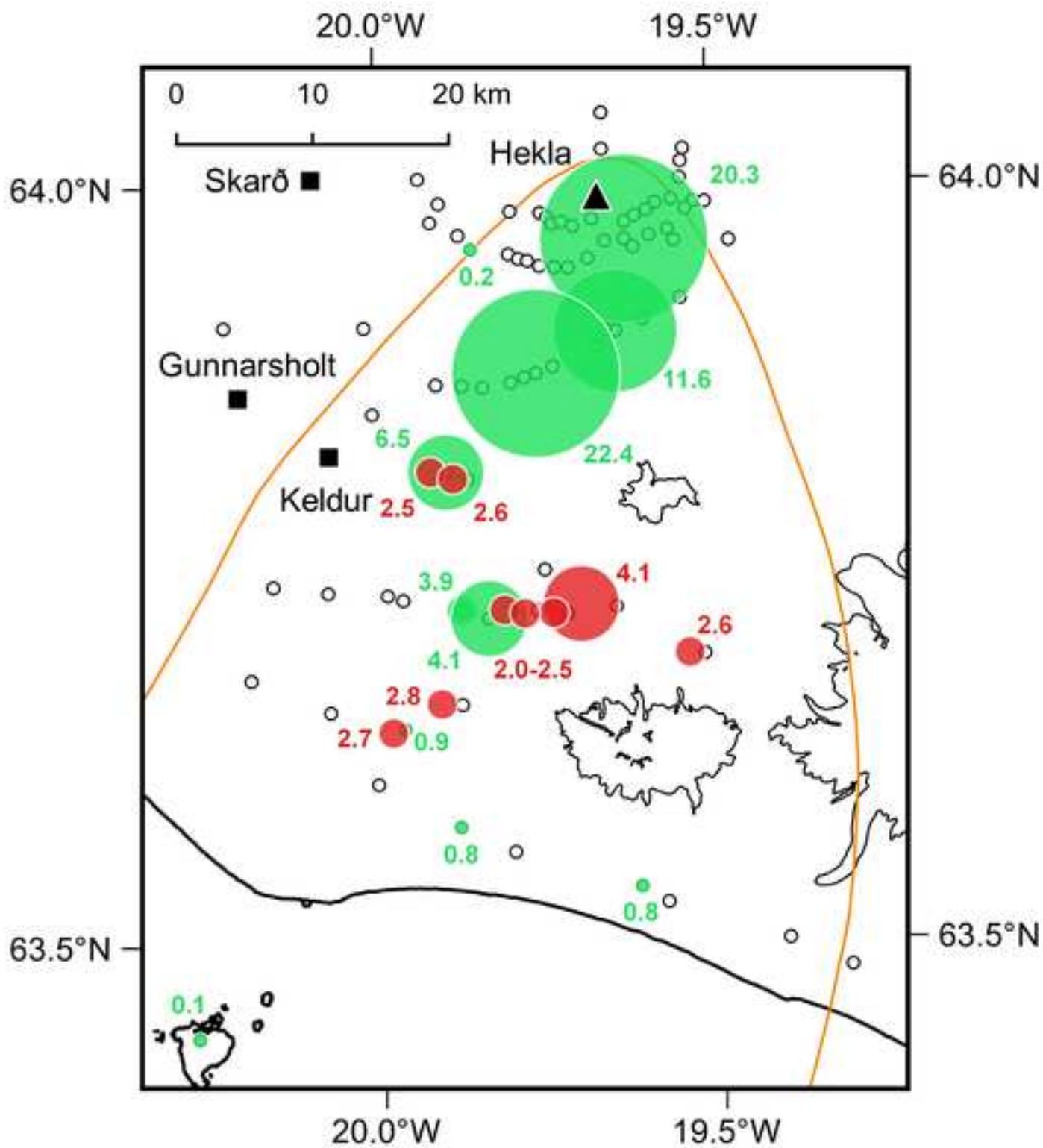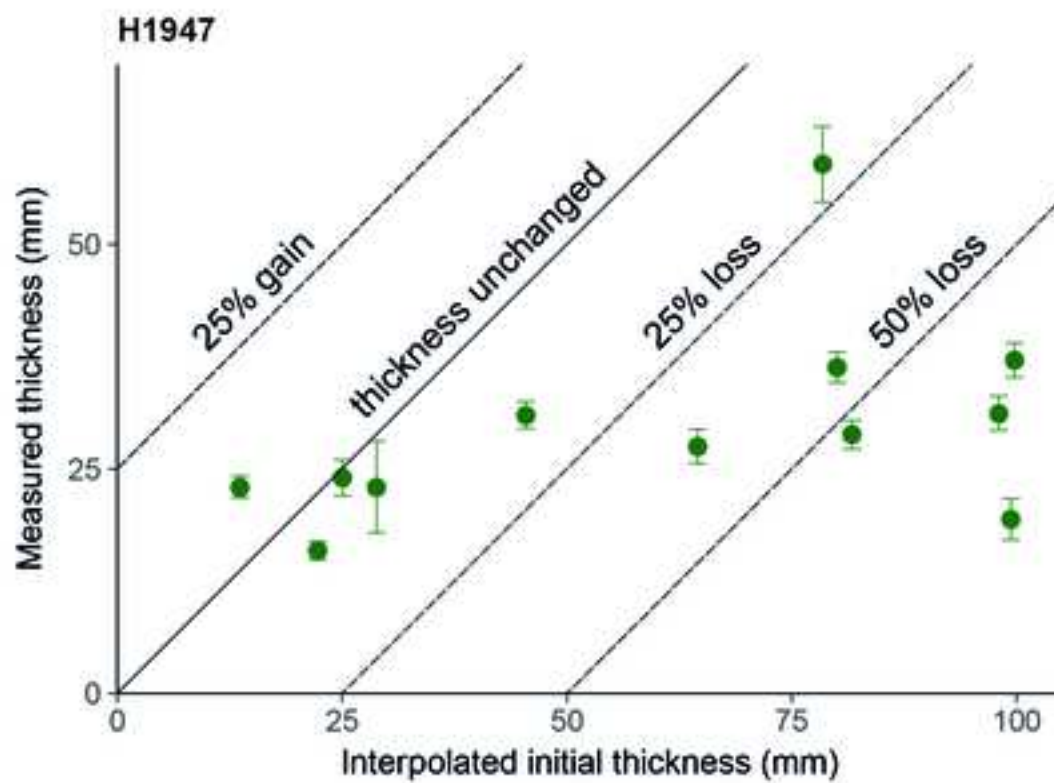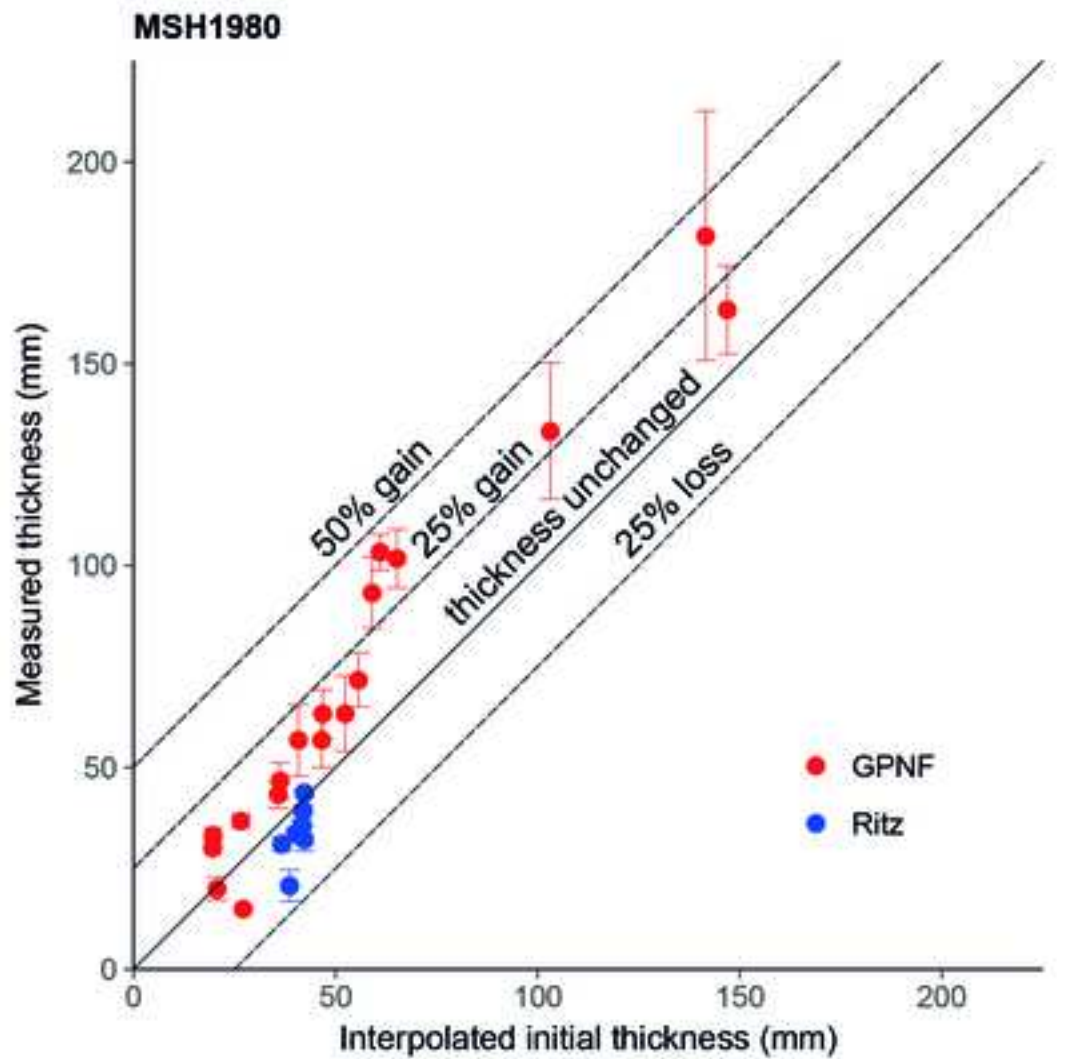
Table 1

Eruption	Date	VEI	Tephra vol. (km^3 DRE)	Area of fallout (km^2)	Thickness half distance (km)	Main source
Hekla 1947 (H1947)	29 March 1947	4	0.045	3130	21.2	Thorarinsson (1954)
Mt St Helens1980 (MSH1980)	18 May 1980	5	0.250	~140,000	34.4	Sarna-Wojcicki *et al*. (1981)

Table 1

Table 2

	Site ID	WGS84 °N	WGS84 °E	distance from vent (km)	mean thickness, T (mm)	T SE (±, mm)	CV in thickness (%)	mass loading (g cm^{-2})
MSH1980	GP01	46.23954	-121.97872	17.5	181.7	30.9	29	NA
	GP02	46.27365	-121.96663	19.8	163.3	10.9	12	NA
	GP04	46.30986	-122.05902	16.8	133.3	16.9	22	NA
	GP05	46.33316	-121.97138	23.3	101.7	7.3	12	NA
	GP06	46.24216	-121.61931	44.7	20.0	2.9	25	NA
	GP07	46.27471	-121.60789	46.2	30.0	0.0	0	NA
	GP08	46.27495	-121.60868	46.1	33.3	1.7	9	1.6
	GP09	46.28448	-121.64542	43.6	36.7	1.7	8	2.8
	GP10	46.29844	-121.68956	40.7	46.7	4.4	16	NA
	GP11	46.29767	-121.71782	38.6	56.7	8.8	27	5.3
	GP12	46.32348	-121.72968	38.7	63.3	6.0	16	7.4
	GP13	46.35586	-121.72059	40.8	63.3	9.3	25	7.3
	GP14	46.36508	-121.72563	41.0	71.7	6.7	16	6.0
	GP15	46.37405	-121.72748	41.3	93.3	8.8	16	11.2
	GP16	46.39465	-121.73271	42.1	103.3	4.4	7	9.5
	GP17	46.42008	-121.75088	42.6	56.7	6.7	20	NA
	GP18	46.43559	-121.76901	42.5	43.3	3.3	13	2.5
	GP19	46.44701	-121.79836	41.7	15.0	0.0	0	NA
	GP20	46.45489	-121.86100	39.0	13.3	4.4	57	NA
	R01	47.09090	-118.66449	288.2	32.3	3.0	16	NA
	R02	47.09590	-118.62557	291.2	43.7	0.9	3	NA
	R03	47.10487	-118.58917	294.1	39.3	1.2	5	NA
	R04	47.10965	-118.55353	296.8	35.7	1.2	6	NA
	R05	47.07618	-118.76224	280.6	33.7	1.2	6	2.3
	R06	47.07300	-118.80140	277.7	20.7	3.9	33	NA
	R07	47.08041	-118.85823	273.9	31.0	1.7	10	NA
H1947	Hk01	61.81116	-19.89899	21.5	19.4	2.3	44	2.5
	Hk02	63.80656	-19.86562	21.3	36.3	1.7	21	2.6
	Hk03	63.68988	-19.51749	33.9	24.0	2.0	37	2.6
	Hk04	63.65824	-19.88710	37.3	31.0	1.5	22	2.8
	Hk05	63.63962	-19.95975	40.4	23.0	1.2	23	2.7
	Hk06	63.72763	-19.95592	31.1	23.0	5.1	65	NA
	Hk07	63.72218	-19.87866	30.4	27.5	1.9	35	NA
	Hk08	63.72272	-19.64339	29.6	58.9	4.2	35	4.1
	Hk09	63.71741	-19.71861	29.6	37.1	1.9	25	2.0
	Hk10	63.71984	-19.79180	29.7	28.8	1.6	28	2.5
	Hk11	63.71721	-19.76161	29.8	31.2	1.9	27	2.1
	Hk12	63.56869	-19.79022	46.4	15.9	1.0	30	NA

Table 2

Click here to access/download
Supplementary Material
ESM_1_rev.pdf

ESM2

ESM3

Click here to access/download
Supplementary Material
ESM_3_rev.pdf

ESM4

Click here to access/download
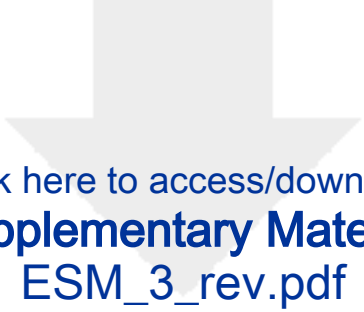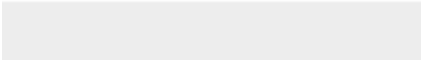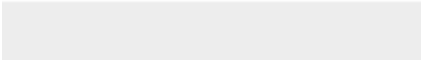Supplementary Material
ESM_4_rev2.pdf

ESM5

Click here to access/download
Supplementary Material
ESM_5_rev.pdf

Click here to access/download
Supplementary Material
ESM_6_rev.pdf

Click here to access/download
Supplementary Material
ESM_7_rev.pdf